Clay-biochar composites for sorptive removal of tetracycline antibiotic in aqueous media

K.S.D. Premarathna[a,b], Anushka Upamali Rajapaksha[a], Nadeesh Adassoriya[a], Binoy Sarkar[c,d], Narayana M.S. Sirimuthu[e], Asitha Cooray[e,f], Yong Sik Ok[g], Meththika Vithanage[a,h,i,*]

[a] Ecosphere Resilience Research Center, Faculty of Applied Sciences, University of Sri Jayewardenepura, Nugegoda, Sri Lanka
[b] Post Graduate Institute of Science, University of Peradeniya, Peradeniya, Sri Lanka
[c] Department of Animal and Plant Sciences, The University of Sheffield, Western Bank, Sheffield, S10 2TN, UK
[d] Future Industries Institute, University of South Australia, Mawson Lakes, SA 5095, Australia
[e] Department of Chemistry, University of Sri Jayewardenepura, Nugegoda, Sri Lanka
[f] Instrument Center, Faculty of Applied Sciences, University of Sri Jayewardenepura, Nugegoda, Sri Lanka
[g] Korea Biochar Research Center, O-Jeong Eco-Resilience Institute & Division of Environmental Science and Ecological Engineering, Korea University, Seoul 02841, Republic of Korea
[h] School of Civil Engineering and Surveying, Faculty of Health, Engineering and Sciences, University of Southern Queensland, West Street, Toowoomba, Queensland, Australia
[i] Molecular Biology and Human Diseases Project, National Institute of Fundamental studies, Kandy 20000, Sri Lanka

ARTICLE INFO

Keywords:
Montmorillonite
Natural red earth
Antibiotics
Intercalation
Composite
Water treatment

ABSTRACT

The focus of this research was to synthesize novel clay-biochar composites by incorporating montmorillonite (MMT) and red earth (RE) clay materials in a municipal solid waste (MSW) biochar for the adsorptive removal of tetracycline (TC) from aqueous media. X-ray Fluorescence Analysis (XRF), Fourier Transform Infrared Spectroscopy (FTIR), Powder X-ray Diffraction (PXRD) and Scanning Electron Microscopy (SEM) were used for the characterization of the synthesized raw biochar (MSW-BC) and clay-biochar composites (MSW-MMT and MSW-RE). Results showed that minute clay particles were dispersed on biochar surfaces. The FTIR bands due to Si-O functional group vibrations in the spectra of the clay-biochar composites provided further evidence for successful composite formation. The kinetic TC adsorption data of MSW-MMT were well fitted to the Elovich model expressing high surface activity of biochar and involvement of multiple mechanisms in the adsorption. The kinetic TC adsorption data of MSW-BC and MSW-RE were fitted to the pseudo second order model indicating dominant contribution of chemisorption mechanism during the adsorption. The adsorption differentiation obtained in the kinetic studies was mainly due to the structure of the combined clay material. The adsorption isotherm data of all the adsorbents were well fitted to the Freundlich model suggesting that the adsorption of TC onto the materials occurred via both physisorption and chemisorption mechanisms. In comparison to the raw biochar and MSW-RE, MSW-MMT exhibited higher TC adsorption capacity. Therefore, MSW-MMT clay-biochar composite could be applied in the remediation of TC antibiotic residues in contaminated aqueous media.

1. Introduction

Aquatic ecosystem pollution via antibiotics is becoming a serious environmental issue. The tetracycline (TC) antibiotics were discovered in 1940s, and started to be used as a therapeutic agent in preserving human heath in 1950s (Eliopoulos and Roberts, 2003). The TC molecule consists of three ionizable functional groups which can protonate and deprotonate, and form different conformations depending on the solution pH (Parolo et al., 2008). Usually at pH < 3.3, cationic form of TC is predominant, at pH 3.3 < pH < 7.7 zwitter ions become dominant, and at pH > 7.7 anionic form becomes dominant (Chang et al., 2014).

Most of the gram negative and gram positive bacteria are vulnerable to antibacterial activity of TC (Abdulghani et al., 2013). Compared to other antibiotics, TC is considered as a cheap antibiotic as a result of which it is popular in developing countries (Roberts et al., 2012). Although the human use of TC has been restricted in many countries due to the development of resistant bacterial strains (López-Peñalver et al.,

2010), it is still extensively used in veterinary medicines as well as a growth promoter in livestock maintenance, poultry farming and aquaculture (Sarmah et al., 2006). When TC is administrated to animals, about 25–75% and 70–90% of the antibiotic are excreted into the environment in active forms via urine and feces, respectively (Halling-Sørensen, 2000). Therefore, antibiotics residues eventually contaminate the soil and surface water via leaching and run off. These residues develop antibiotic resistance to microorganisms, inhibit growth of some aquatic species, and directly influence the steroidogenic pathway which leads to endocrine disruption in humans (Halling-Sørensen, 2000; Daghrir and Drogui, 2013; Ji et al., 2010). A study in Sri Lanka showed that effluents released from poultry and livestock farms contained approximately 45, 35 and 20% of TC, oxytetracycline (OTC) and amoxicillin (AMX), respectively (Liyanage and Manage, 2017). The average concentration ranges of TC, OTC and AMX in effluents of selected poultry farms are 0.001–0.005, 0.001–0.004 and 0.001–0.005 mgL^{-1} (Liyanage and Manage, 2017).

Therefore, it is necessary to eliminate TC residues from effluents prior to their release in the environment. Compared to current water treatment techniques available, such as membrane processes, photochemical processes, electrochemical processes, photocatalytic and photoelectrocatalytic processes, ozonation and advanced oxidation (Košutić et al., 2007; Koyuncu et al., 2008; Chen et al., 2010; Lee et al., 2011), adsorption is considered as a simple, cost effective, and less harmful technique for the removal of TC from waste water. Different types of adsorbents have been used for the adsorptive removal of antibiotics of all categories, but not TC (Chang et al., 2016; Rajapaksha et al., 2015). Most of the adsorbents used in adsorption studies are abundant, naturally originated and relatively cheap, such as biochar and clays (Ahmad et al., 2014; Uddin, 2008).

Biochar is a porous carbonaceous material with large specific surface area, and it is produced via pyrolysis of biomass in sealed containers, under limited oxygen environment (Lehmann and Joseph, 2009). The initial use of biochar was limited to the enhancement of agricultural productivity via improvement of soil fertility, increasing soil nutrient levels and water retaining capacity, and decreasing greenhouse gas emission through carbon sequestration (Lehmann and Joseph, 2009; Mandal et al., 2016). However, in recent years, biochar has been used as a cost effective adsorbent for immobilizing both organic (antibiotics, pesticides, dyes) and inorganic contaminants (nutrients, heavy metals) (Vithanage et al., 2014, 2016; Yang et al., 2016; Yao, 2013; Han et al., 2013). Biochar can be produced using various feedstocks, mainly crop residues and waste biomasses, which are abundant and easily collectable, and considered as waste materials, hence indirectly supporting sustainable waste management (Ahmad et al., 2014).

Montmorillonite (MMT) is the most commonly used clay mineral as an adsorbent for the removal of variety of contaminants (Aristilde et al., 2016; Zhu et al., 2016; Krupskaya et al., 2017). It is an aluminosilicate clay mineral with 2:1 type structure in which aluminum and silicon are the main components of layers, and one aluminum octahedral sheet is stacked in-between two silicon tetrahedral sheets (Krupskaya et al., 2017). Negatively charged layers in the clay mineral are balanced by hydrated exchangeable cations (Na^+, Ca^{2+}, Mg^{2+}) present in the interlayer space (Segad et al., 2010). Cations present in the interlayer space of MMT can exchange with positively charged contaminants via cation exchange mechanism (Yao, 2013). Such a cation exchange reaction is a physical mechanism which is referred to as intercalation when guest ions or molecules occupy the interlayer space by replacing the hydrated cations (Aristilde et al., 2016; Li et al., 2010; Perelomov et al., 2016).

Natural red earth clay (RE) is an iron coated quartz sand consisted of small amounts of ilmenite and magnetite, and abundantly found in the northwest coast of Sri Lanka covering the lime stone strata (Vithanage et al., 2007). According to available literature, RE mainly consists of silica (SiO_2) coated with considerable concentrations of Al_2O_3 and Fe_2O_3 (Vithanage et al., 2006, 2007). The Fe^{2+} level is comparatively high, and sometimes reaches up to 6%, and both aluminum and iron (> AlOH and > FeOH) act as active surface sites. As a result, the surface charge of RE can be varied with variation of pH in the surrounding environment. Although RE did not show porous or layered structure (Vithanage et al., 2007), it could have high adsorption capacity for heavy metals and metalloids like arsenic and nickel (Vithanage et al., 2006; Rajapaksha et al., 2011, 2012). However, previously RE clay was not used to determine its adsorption affinity for antibiotics likely due to the non-layered structure and low surface activity of the material.

Compared to activated carbon, biochar was found less promising in the context of adsorptive removal of contaminants from aqueous media because of the relatively low surface area of the latter material, and the influence of abiotic and/or biotic processes on its properties and adsorption capacity (Anderson et al., 2013). Hence, biochar composites prepared by impregnating biochar with specific materials such as clay minerals have been tested for the adsorption of contaminants like antibiotics and nutrients (Yao et al., 2014; Li et al., 2017; Chen et al., 2017). For instance, in biochar-clay composites, biochar could provide surfaces for the distribution of the clay particles (Yao et al., 2014), and thus improve contaminant adsorption capacity of the pristine material.

Nevertheless, the application of clay-biochar composites for antibiotic removal from aqueous media and associated mechanisms have seldom been investigated to the best of our knowledge. Therefore, current study was conducted to investigate the TC adsorption behavior of two different clay-biochar composites prepared by incorporating MMT and RE in municipal solid waste (MSW) derived biochar, and discuss the mechanisms involved in the adsorption of TC by these composites. The raw biochar and clay-biochar composites are henceforth referred as MSW-BC, MSW-MMT and MSW-RE, respectively.

2. Materials and methods

2.1. Clay-biochar composite preparation

Stable suspensions of MMT and RE were prepared independently (50 g clay in 2 L deionized (DI) water), and the mixtures were sonicated for 30 min in an ultrasonicator (Rocker). Then 250 g of MSW feedstock prepared by processing municipal solid waste collected from waste disposal sites was added to each of the clay suspensions, and the mixtures were shaken for 2 h in a shaker at 100 rpm speed. Clay-MSW feedstock suspensions were filtered to remove the liquids, and the solid materials were dried at 80 °C overnight in a hot air oven. The clay-treated biomass feedstocks were packed tightly to ceramic crucibles and pyrolyzed at 500 °C for 30 min under oxygen-limited environment in a muffle furnace (MTI, Richmond, CA). Untreated MSW feedstock was also pyrolyzed under the same pyrolysis conditions for the production of raw biochar. All the biochar and clay-biochar composite samples were washed several times with DI water to remove soluble impurities, then kept in an oven at 80 °C for drying, and finally sealed in a container for further experimental use.

2.2. Material characterization

Surface physical morphology and microstructure of the clay-biochar composites were determined by Field Emission Scanning Electron Microscopy (Hitachi SU6600 Analytical Variable Pressure FE-SEM). Structure and crystallinity of the composite materials before and after adsorption of TC were determined by Powder X-ray Diffraction (PXRD) on a Rigaku, Ultima IV X-ray Diffractometer (Japan) using Cu Kα radiation (λ = 1.54056 Å). Surface chemical properties of the raw biochar and clay-biochar composites were analyzed before and after adsorption of TC using a Fourier Transform Infrared Spectrometer (Thermo scientific Nicolet iS10, USA). The Elemental Analysis was done by using a X-ray Fluorescence (XRF) analyser. Electrical Conductivity

Table 1
Elemental analysis and basic chemical characteristics of MSW-BC, clay materials (MMT and RE) and clay-biochar composites (MSW-MMT and MSW-RE).

Sample	Mg%	Al%	Si%	P%	S%	K%	Ca%	Ti%	Mn%	Fe%	pH	EC μScm^{-1}	BET Surface area m^2 g^{-1}
MSW-BC	ND	9.12	49.58	10.65	3.88	9.52	12.99	0.96	ND	3.30	9.55	3320	4.33
MMT	5.04	15.83	66.85	ND	0.35	0.96	2.45	0.29	0.03	8.20	7.56	1675	–
RE	ND	11.66	75.78	ND	0.06	0.58	ND	2.94	ND	8.78	7.13	298	–
MSW-MMT	ND	8.66	46.4	2.08	1.66	ND	20.13	0.86	0.17	8.84	9.51	1799	8.72
MSW-RE	ND	12.76	44.26	ND	ND	7.39	12.29	2.97	0.25	19.51	8.99	1049	8.44

(EC) and pH of the materials in aqueous suspensions were measured using an Electro-Conductivity meter (ORION 210A) and a pH meter (ORION 210A), respectively.

2.3. Sorption-edge experiments

The impact of pH on the adsorption of TC by the adsorbents was studied in a pH range of 3.0–9.0. Adsorbent concentrations (MSW-BC, MSW-MMT and MSW-RE) were kept at 2.00 gL^{-1} in the solutions containing TC 20.00 mgL^{-1}. Then pH was adjusted with 0.1 M HNO_3 or NaOH. Adsorbent-adsorbate systems were equilibrated in a shaker at a rate of 100 rpm for 12 h, and final pH of samples were measured. Thereafter, suspensions were filtered through syringe filters of 0.45 μm, and TC concentrations in the clear solutions were measured at 268.6 nm wavelength using a spectrophotometer (Shimadzu UV160A). Two replicates were done for each pH.

2.4. Kinetic experiments

In the kinetic experiment, adsorbent concentrations (MSW-BC, MSW-MMT and MSW-RE) were kept 2.00 gL^{-1}, and the TC concentration was taken 20.00 mgL^{-1} of TC. The pH of the system was maintained in 7.0–8.0 range. Suspensions were withdrawn from the shaker at various time intervals: 5, 10, 20, 30 min, and 1, 2, 4, 6, 10 and 24 h. The pH of the suspensions were measured at each sampling occasion. Then, suspensions were filtered through 0.45 μm syringe filters, and TC concentrations in the clear solutions were measured at 268.6 nm wavelength using a spectrophotometer (Shimadzu UV160A). Two replicates were done for each contact time. Kinetic modeling was done using the Origin Ver. 6.1 software package. The pseudo second order (Eq. (1)), pseudo first order (Eq. (2)) and Elovich (Eq. (3)) equations (Ho and McKay, 1998a, 1998b, 2002) were used for data modeling.

$$\text{Pseudo second order model: } \frac{dq_t}{dt} = k_2(q_e - q_t)^2 \quad (1)$$

$$\text{Pseudo first order model: } \frac{dq_t}{dt} = k_1(q_e - q_t) \quad (2)$$

$$\text{Elovich equation: } \frac{dq_t}{dt} = \alpha exp\,(-\beta q_t) \quad (3)$$

where, amount of adsorbed TC at equilibrium and time 't' are q_e (mg g^{-1}) and q_t (mg g^{-1}), respectively; equilibrium rate constants are k_1 (min^{-1}) and k_2 (g mg^{-1} min^{-1}), initial adsorption rate is α (mg g^{-1}min^{-1}); and desorption constant is β (g mg^{-1}).

2.5. Isotherm experiments

Adsorption isotherms were determined in a TC concentration range of 0.25–250.00 mg L^{-1} using an adsorbent dose of 2.00 gL^{-1}, and pH was maintained in the 7.0–8.0 range throughout the experiment. After contact time of 6 h (as observed from the kinetic experiment that TC adsorption equilibrium reached in this duration), the pH values of the suspensions were measured, and TC concentrations in the clear solutions were analyzed, as described previously. Isotherm data for adsorption of TC by MSW-BC, MSW-MMT and MSW-RE were modeled using the Langmuir (Eq. (4)), Freundlich (Eq. (5)) and Temkin (Eq. (6)) isotherm models.

$$\text{Langmuir isotherm model: } q_e = \frac{Q_{max}\ K_L\ C_e}{1 + K_L C_e} \quad (4)$$

$$\text{Freundlich isotherm model: } q_e = K_f C_e^n \quad (5)$$

$$\text{Temkin isotherm model: } qa_{ads} = RT\frac{(\ln AC_e)}{b} \quad (6)$$

where, K_f (mg g^{-1} (mg L^{-1})$^{-n}$, K_L (L mg^{-1}) are the Freundlich and Langmuir affinity parameters, A and b are constants for Temkin model, q_e (mg g^{-1}) is the equilibrium adsorption capacity, q_{ads} (mg g^{-1}) is the equilibrium adsorption capacity of Temkin model, C_e (mg L^{-1}) is the equilibrium liquid phase concentration, Q_{max} (mg g^{-1}) is the maximum adsorption capacity in Langmuir model, n is a Freundlich constant related to adsorption, R and T (K) are the universal gas constant and absolute temperature, respectively.

3. Results and discussion

3.1. Adsorbent characterization

The elemental compositions of the raw biochar and clay-biochar composites are presented in Table 1. The percentage of Si and Al in MSW-MMT and MSW-RE clay-biochar composites did not increase with the clay modification of MSW-BC. It was likely because the amounts of Si and Al were added to the feedstock in the form of MMT and RE were negligible in comparison to the original amounts of these elements already present in MSW. Hence, XRF analyser was unable to detect the concentration differences of Al and Si in the adsorbent materials.

Nevertheless, percentages of Fe in both the composites were higher than MSW-BC, and much higher in MSW-RE composite due to the high Fe content in the pristine RE clay. All other elements in the clay-biochar composites were generally low in contents and comparable with each other (Table 1). The pH of the raw biochar (MSW-BC) was basic in nature (pH = 9.55) due to the organic nature of MSW feedstock. The pH of MSW-MMT composite was not much different (pH = 9.51) than the raw biochar due to the predominance of biochar pH and less acidity of the MMT clay mineral (pH = 7.56) (Chen et al., 2017). However, the pH of MSW-RE clay-biochar composite was significantly lower (pH = 8.99) than MSW-MMT due to the low pH of the original RE clay (pH = 7.13). Electrical conductivity of the clay-biochar composites was decreased with clay modification in contrast to MSW-BC due to the high metal contents in the clay materials used (Table 1). The BET surface areas of the two clay-biochar composites were almost as double as that of the MSW-BC, may be because of the deposition of clay particles on the surface of MSW-BC.

The FTIR spectra of both MSW-MMT and MSW-RE clay-biochar composites showed considerable differences compared to MSW-BC (Fig. 1). The bands observed around 1030 - 1040 cm^{-1} pointed towards the introduction of Si-O functional groups onto the MSW-MMT and MSW-RE surfaces (Chen et al., 2017). The bands appearing below 1100 cm^{-1} might be attributed to Si—O stretching, Si-O-Si bending, Si-O-Al bending and Si-O-Mg bending vibrations (Chen et al., 2017). Some of these bands were detected in the IR spectra of the clay-biochar composites. The above observations provided evidences for the

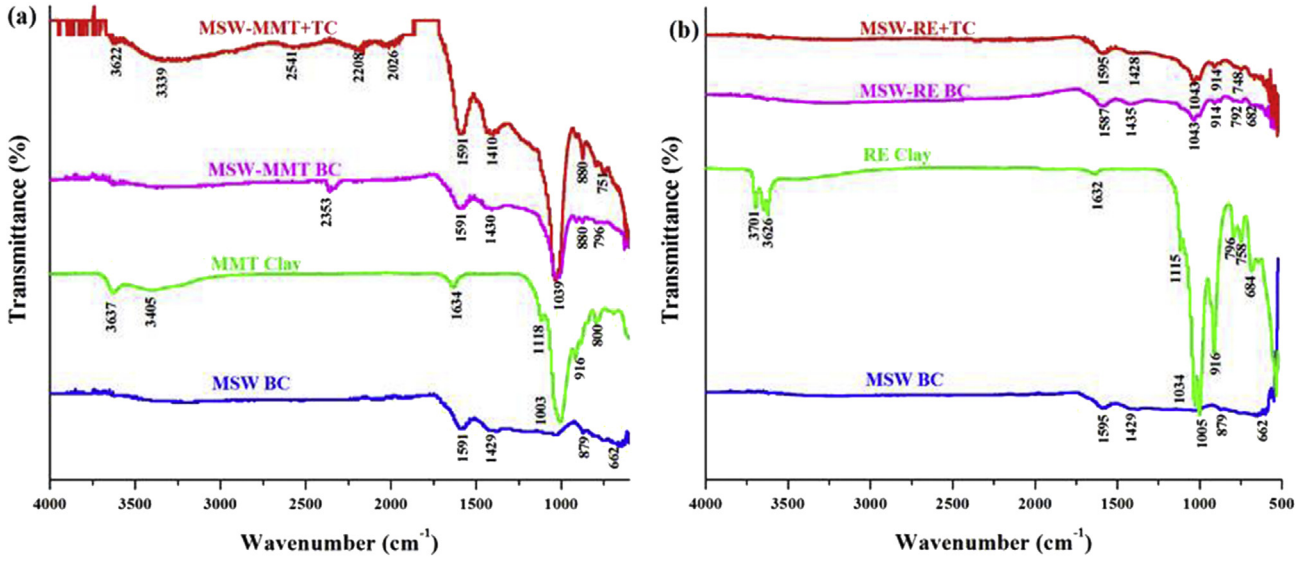

Fig. 1. FTIR spectra of biochar and clay-biochar composites: (a) MSW-MMT composite before and after adsorption of TC, and (b) MSW-RE composite before and after adsorption of TC.

successful formation of clay-biochar composites.

As given in Fig. 2a, PXRD pattern of MSW-MMT composite showed six major X-ray reflections at 2θ values 5.75° (d = 1.53 nm), 17.40° (d = 0.51 nm) 19.79° (d = 0.45 nm), 26.52° (d = 0.34 nm), 28.60° (d = 0.31 nm) and 34.90° (d = 0.26 nm). All the reflections from the parent MMT clay mineral were present in MSW-MMT composite. The primary reflection observed at 2θ = 5.75° both in MMT and MSW-MMT corresponded to a basal spacing (d_{001}) of 1.53 nm. In the PXRD patterns of both RE clay and MSW-RE composite, primary reflections were observed at 2θ = 12.18° ($d_{0.01}$ = 0.73 nm) (Fig. 2b).

The SEM images of MSW-MMT and MSW-RE clay-biochar composites are shown in Fig. 3. Pores were observed on biochar surfaces, which could support TC removal via enhancing surface adsorption with the increase of surface area and through pore filling mechanism. The SEM images of both clay-biochar composites clearly showed clay particles adhering on to the biochar surfaces, which gave the biochar surfaces much rough appearance and provided more reactive surface area for adsorption than the pristine biochar. However, clay particles did not cover the entire surface of biochar, and kept the pores of biochar accessible to the adsorbate molecules. An excessive coating with clay particles rather could cause an obstruction of pores, and ultimately might lead to a decrease of adsorption capacity of the composite adsorbent (Yao et al., 2014; Fosso-Kankeu et al., 2015).

3.2. pH edge experiments

The pH of the solution is a major factor that controls antibiotic adsorption on to biochar and clay-biochar composites (Li et al., 2017). The solution pH also has influences on the molecular form of antibiotics and surface charge of adsorbents depending on the pH_{pzc} of the solid phases (Chang et al., 2016). According to Fig. 4, the adsorbed amount of TC was gradually increased with an increase of pH. The highest TC adsorption by MSW-BC was exhibited at pH 5.0, and the highest TC adsorption by MSW-MMT and MSW-RE composites were observed at pH 7.0. As compared to MSW-BC and MSW-RE, MSW-MMT showed a significant increase of TC adsorption at all the pH values studied between pH 3.0 and 9.0 (Fig. 4). A NaOH-activated biochar previously produced using *Pinus taeda* showed similar trend in adsorption capacities at pH 3.0–9.0 range, and the maximum adsorption capacity was obtained at pH 5.0 (Jang et al., 2018). The TC adsorption capacities of

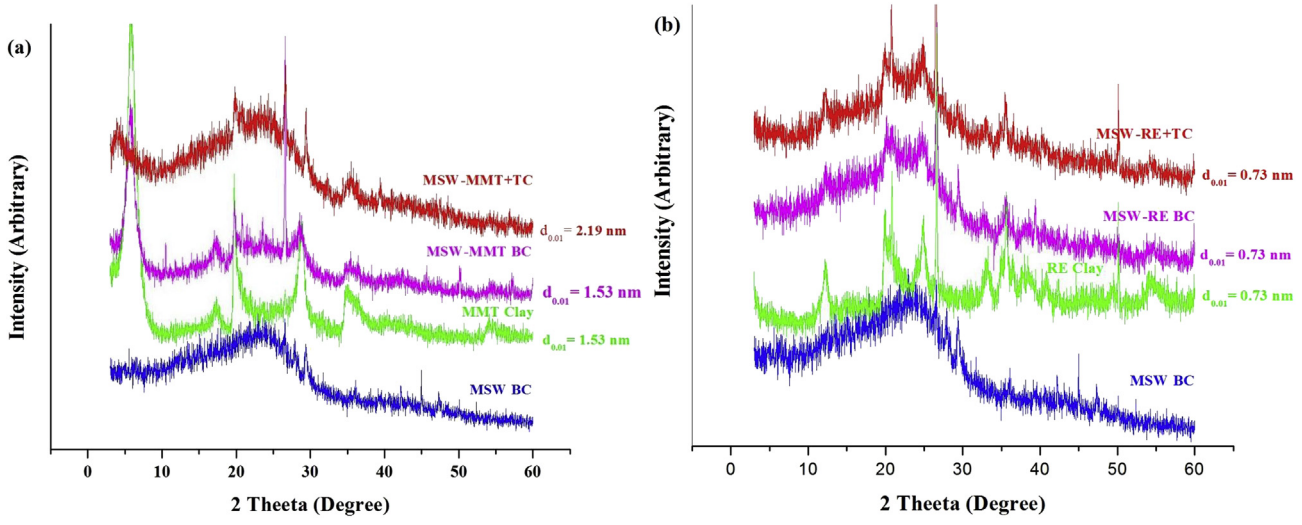

Fig. 2. PXRD patterns of biochar and clay-biochar composites: (a) MSW-MMT composite before and after adsorption of TC, and (b) MSW-RE composite before and after adsorption of TC.

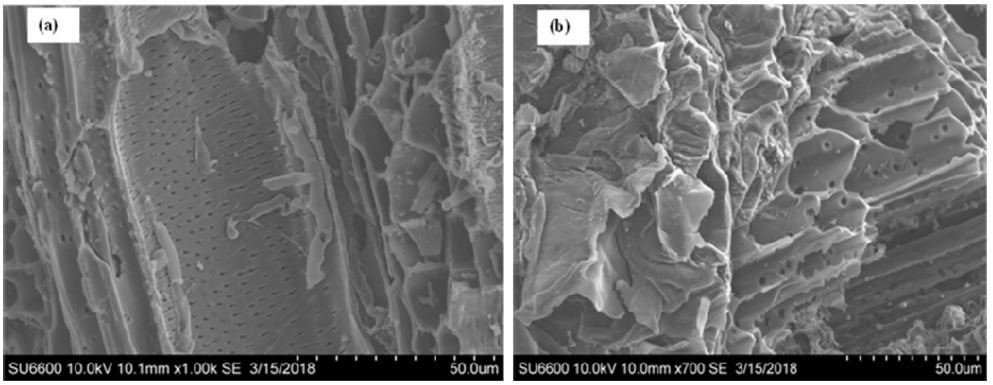

Fig. 3. SEM images of clay-biochar composites: (a) MSW-MMT composite, and (b) MSW-RE composite.

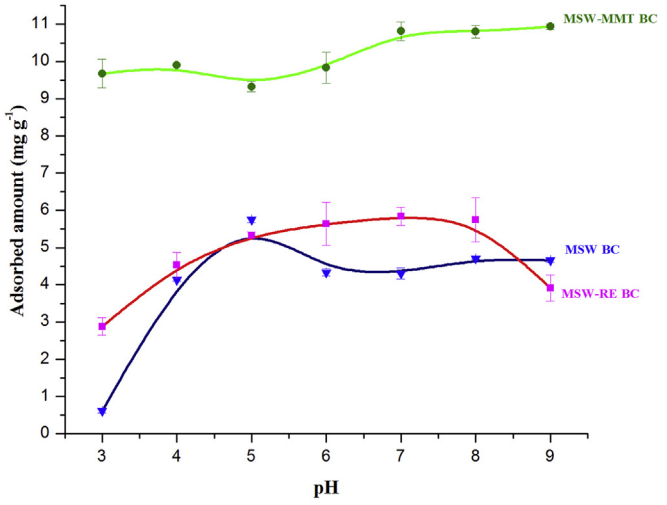

Fig. 4. pH vs TC adsorption capacities of MSW-BC, and MSW-MMT and MSW-RE composites.

other modified biochars (P-biochar, Fe-biochar, Zn-biochar, and Fe/Zn-biochar) exhibited comparable trend, and their adsorption capacities were at the peak at pH 6.0 and then gradually decreased with further increase of pH (Zhou et al., 2017). Decrease of adsorption capacities of TC at high pH values may be resulted due to electrostatic repulsion caused by negatively charged TC and surface of the biochar on which elevated negative charge density formed above pH_{pzc} (Rivera-Utrilla et al., 2013). However, H_3PO_4-modified rice straw and swine manure biochars showed the maximum adsorption capacity at pH 9.0, and adsorption capacities of both the biochars were relatively high at pH between 5.0 and 9.0, and hence elevated adsorption at alkaline pH mainly depended on pH_{pzc} of the modified biochars (Chen et al., 2018).

3.3. Kinetic experiments

Adsorption capacities of all the adsorbents for TC were increased rapidly at the initial stage, followed by a slow increase, and then reached equilibrium within 6 h (Fig. 5a). However, compared to MSW-BC and MSW-RE, MSW-MMT showed a higher TC adsorption capacity. Such a significant enhancement of adsorption capacity of TC by MSW-MMT could be due to the superior ion exchange capacity of the layered MMT clay mineral (Yao et al., 2014).

The adsorption kinetic data of MSW-BC and MSW-RE were fitted to the pseudo second order model with r^2 values of 0.929 and 0.978, respectively (Table 2), which can be further confirmed by the excellent closeness of the calculated q_e values ($q_{e.cal}$) from the modelled and experimental q_e value ($q_{e.exp}$) obtained from the graph for MSW-BC ($q_{e.cal}$ = 3.921, $q_{e.exp}$ = 3.937) and MSW-RE biochar ($q_{e.cal}$ = 4.156, $q_{e.exp}$ = 4.131). The rate constant value of MSW-RE composite obtained from the pseudo second order kinetic model was slightly higher than that of MSW-BC (Table 2). Hence, MSW-BC and MSW-RE adsorbed TC mainly via surface adsorption which could involve chemisorption (Wang et al., 2007). The rate-limiting step could be a chemisorption process or chemical reaction which might involve electron sharing or exchange among TC and the adsorbents. Therefore, it could be suggested that the adsorption of TC onto MSW-BC and MSW-RE occurred via chemical interactions, and a long time was required to reach the equilibrium. Kinetic data fitting to Elovich model indicated that MSW-MMT composite had a high surface activity for TC adsorption, and an enhanced surface coverage decreased the adsorption rate with time (Chen et al., 2017). Therefore, the adsorption could occur via multiple mechanisms. The mechanisms of adsorption of TC onto MSW-MMT composite might be dominated by intercalation interaction and chemical reactions occurring between the adsorbent surface and TC.

3.4. Isotherm experiments

The Freundlich isotherm model was the best fitted model for isotherm data of MSW-BC, MSW-MMT and MSW-RE (Fig. 5b) with r^2 values of 0.994, 0.973 and 0.949, respectively (Table 3). Hence, the adsorption of TC occurred on to heterogeneous surfaces of the adsorbents, and the adsorption was a multilayer process (Yao, 2013). These results were in alignment with kinetic modeling results that the adsorption could occur via multiple mechanisms. The PXRD analysis also indicated multiple TC adsorption mechanisms including intercalation of TC in MMT interlayers of the clay-biochar composite. Therefore, adsorption could occur via both chemisorption and physisorption. The Langmuir maximum adsorption capacity of TC on MSW-MMT composite was 78 mg g^{-1}. Such a high TC adsorption capacity of MSW-MMT could be due to the intercalation interactions occurring between TC and MMT particles dispersed on the surface of the biochar.

Biochar as well as biochar composites prepared by various modifications were earlier used for the sorptive removal of TC in water (Jing et al., 2014). Rice husk biochar and methanol modified rice husk biochar were used for the absorptive removal of TC. Raw rice husk biochar prominently removed TC via π-π interactions occurring between aromatic rings of TC and biochar, whereas modified biochar showed 45.6% enhancement in TC adsorption capacity (Jing et al., 2014). However, coconut shell biochar showed considerably lower adsorption capacity for TC (100 μg g^{-1}), whereas TC adsorption capacity of bamboo biochar almost equalled to the TC adsorption capacity of graphene (approximately 200 μg g^{-1}), and the adsorption was mainly depended on π-π interactions (Peng et al., 2016).

Sludge-derived materials were also used to remove TC from water. The capacity of these materials to adsorb TC was very high and was much greater than that of commercial activated carbon. Such elevated adsorption capacity (512.1–672.0 mg g^{-1}) is explained by the high

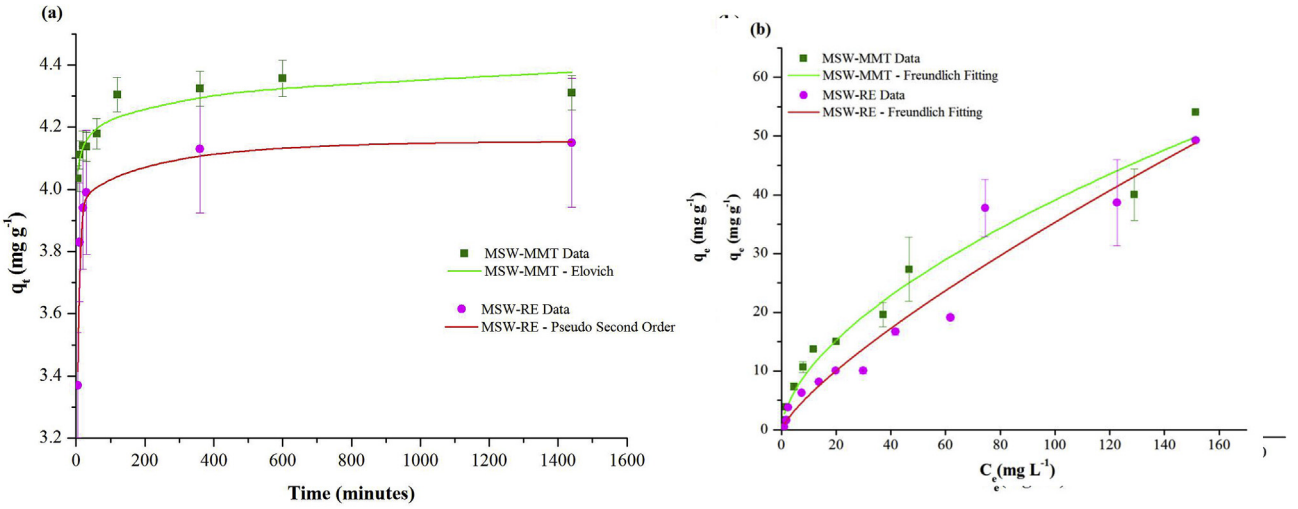

Fig. 5. (a) Kinetic data models for the adsorption of TC by MSW-MMT and MSW-RE clay-biochar composites, and (b) adsorption isotherm fittings for MSW-MMT and MSW-RE composites to the Freundlich model. The symbols correspond to experimental results at pH range 7.0–8.0, and the solid lines symbolize the calculated results obtained from the non-linear curve fitting.

Table 2
Kinetic parameters acquired from pseudo-first-order, pseudo-second-order and Elovich models of TC adsorption onto MSW-BC, MSW-MMT and MSW-RE adsorbents.

Model	Parameters	MSW-BC	MSW-MMT	MSW-RE
Pseudo first order	k_1(min^{-1})	0.268	0.284	0.350
	q_e(mg g^{-1})	3.743	8.046	4.039
	r^2	0.658	0.432	0.901
	RMSE	–	–	–
Pseudo second Order	k_2[g (mg min)$^{-1}$]	0.130	0.061	0.221
	q_e(mg g^{-1})	3.921	8.386	4.156
	r^2	0.929	0.747	0.978
	RMSE	0.225	1.343	0.3845
Elovich	α_E[mg (g·min)$^{-1}$]	557,234	398,561	–
	β_E(g mg^{-1})	5.279	2.319	
	r^2	0.896	0.886	

tendency of TC to form complex ions with some of the metal ions present in these materials (Rivera-Utrilla et al., 2013). The medium pH and presence of electrolytes considerably affected TC adsorption on commercial activated carbon. These results indicate that electrostatic adsorbent- adsorbate interactions play an important role in TC adsorption processes when conducted at pH values that produce TC deprotonation.

Activated carbon is a most frequently utilized adsorbent for the remediation of antibiotic residues present in the environment. Lignin-activated carbon showed higher adsorption capacity (475.48 mg g^{-1}) for TC in aqueous media (Huang et al., 2014). High surface area, porous structure and availability of acidic and basic functional groups were responsible for this enhanced adsorption. The adsorption of TC by MMT clay mineral was influenced by the presence of different multivalent metal ions, such as Ca^{2+}, Mg^{2+}, Cu^{2+}, Al^{3+} and Fe^{3+} in the medium (Aristilde et al., 2016). In alkaline medium, presence of these metal ions promotes formation of bridges between negatively charged groups of TC and the negatively charged surface of clay minerals via covalent bonding.

3.5. Tetracycline removal ability and adsorption mechanisms

According to the experimental results, MSW-MMT composite enhanced the TC adsorption capacity in comparison to the raw biochar and MSW-RE composite. This enhancement could be justified by the presence of additional functional groups which were not detected in the FTIR spectrum of MSW-MMT composite prior to TC adsorption (Fig. 1a), and except thier presence in the FTIR spectrum of TC antibiotic (Fig. S1). For example, bands appeared at around 3339 cm^{-1} (O—H stretching), and 2026, 2208 and 2541 cm^{-1} due to carbon-carbon triple bond stretching (Li et al., 2017). However, MSW-RE composite after adsorption of TC did not show these additional bands, but they were observed in MSW-RE before TC adsorption, which might be due to the low affinity exhibited by MSW-RE for TC.

Adsorption isotherm results concluded that the adsorption occurred via both physisorption and chemisorption. However, results signified that physisorption was the dominant contributor towards the high TC adsorption capacity shown by MSW-MMT. During physisorption, biochar could interact with TC physically via pore-filling mechanism and intercalation interaction. At pH $<$ 4.0, positively charged form of TC is dominant which could reach the interlayer space of clay minerals by exchanging with the hydrated cations (Na^+, Ca^{2+}) residing in the inter layer space. At the pH range of 4.0–8.0, zwitterionic form of TC is the dominant species which also could penetrate into the interlayer space between two t-o-t layers of the clay mineral. The PXRD pattern of MSW-MMT composite was changed and the primary reflection of MMT in the PXRD pattern shifted to 2θ = 4.03° corresponding to a basal spacing value ($d_{0.01}$) of 2.19 nm (Fig. 2a), which was higher compared to $d_{0.01}$ before the adsorption (1.53 nm). This could be attributed to the

Table 3
Langmuir, Freundlich and Temkin isotherm parameters for the adsorption of TC onto MSW-BC, MSW-MMT and MSW-RE adsorbents.

Model	Langmuir			Freundlich			Temkin		
Parameter	K(L mg^{-1})	Q_{max}(mg g^{-1})	r^2	K_f(mg g^{-1})/(mg L^{-1})^n	n	r^2	A	b	r^2
MSW-BC	–	–	–	0.143	1.191	0.994	4.1×10^{-4}	2.937	0.983
MSW-MMT	0.0149	77.962	0.958	3.043	0.586	0.973	5.4×10^{-4}	2.530	0.563
MSW-RE	–	–	–	0.963	0.782	0.949	4.2×10^{-4}	3.006	0.923

adsorption of TC on to the clay-biochar composite via TC intercalation into the inter-layer space of MMT clay mineral. Fig. 2a provided evidence for intercalation interactions occurring between MMT particles present on the biochar surface and TC. Aristilde (Aristilde et al., 2016) and Chang (Chang et al., 2014) also observed the expansion of inter-layer space after adsorption of TC on to MMT clay mineral. At pH > 8.0, the dominant form of TC is anionic, which would electrostatically repel the negatively charged clay surfaces resulting in a decreasing trend of the adsorption capacity above pH 8.0. Although, physisorption dominated, chemisorption via chemical bonding and enhancement of available binding area resulted by deposition of MMT on biochar surfaces also facilitated adsorption.

The clay-biochar composite prepared from RE showed adsorption capacities similar to MSW-BC. Although the BET surface areas of both biochar composites were almost the same, the TC adsorption capacity of MSW-RE was very low compared to MSW-MMT, which might be due to the non-layered structure of RE clay (Vithanage et al., 2007). Unchanged $d_{0.01}$ of MSW-RE composite even after adsorption of TC indicated no intercalation of TC in case of MSW-RE, but a possible surface adsorption process via enhanced surface area of biochar composites occurred due to deposition of clay particles on biochar surfaces. For both raw biochar and MSW-RE composite, adsorption is dominated via chemical interactions such as π-π interaction, because of the availability of aromatic rings, then via hydrogen bonding, ion exchange and electrostatic interactions. Physical adsorption via pore filling mechanism is also possible as a result of porous nature of biochar. However, at high pH level, adsorption capacities of TC decreased for the biochar, which may be resulted due to electrostatic repulsion occurring between negatively charged TC and surface of the negatively charged biochar above pH_{pzc} (Jang et al., 2018).

Finally, according to the obtained results, MSW-MMT composite exhibited higher adsorption capacity for TC, whereas MSW-BC and MSW-RE showed much lower adsorption capacity. Although, MSW-RE biochar composite was successfully prepared, the RE clay was unable to improve adsorption capacity significantly compared to MMT clay mineral. However, these clay materials are naturally occurring materials in the environment and highly abundant, therefore use of clay-modified biochar is a better way to enhance adsorption ability of biochar via simple procedure.

4. Conclusions and future perspectives

Two novel clay-biochar composites were prepared by pyrolysis of MSW biomass mixed with MMT and RE clay materials. Minute clay particles were observed on the surfaces of biochar in the clay-biochar composites, and the IR bands due to Si-O vibration were observed in the spectra of the composites, which provided evidence for successful composite formation. The PXRD patterns gave evidence of intercalation interaction occurring between MMT and TC in the case of MSW-MMT composite by increasing the basal spacing of the clay mineral after adsorption of TC. The adsorption of TC was higher at basic pH values for all the adsorbents than acidic pH range. The MSW-MMT showed significantly higher TC adsorption capacity compared to MSW-BC and MSW-RE at a pH range of 3.0–9.0.

The adsorption kinetic data of MSW-MMT fitted to the Elovich model, and that of MSW-BC and MSW-RE fitted to the pseudo second order model. The Freundlich model best fitted the adsorption isotherm data for all the adsorbents indicating that the adsorption was a multilayer process involving both physisorption and chemisorption, especially for MSW-MMT composite. Results implied that high surface activity, surface area and interlayer spaces provided by the layered MMT clay mineral improved TC adsorption capacity of MSW-MMT composite via both surface adsorption and intercalation interactions, whereas the raw MSW-BC and MSW-RE did not show any intercalation interaction. Thus, MSW-MMT was an effective adsorbent over MSW-RE and MSW-BC for the removal of TC antibiotic residues from aqueous media.

In addition, the use of MSW for the production of biochar contributed to sustainable urban waste management. However, in certain instances, the use of MSW biochar may contain compounds that can potentially interfere with the adsorption of target contaminant by altering its structure (e.g., TC antibiotic). Use of such biochar for the adsorption of antibiotics is not effective. Adsorption studies are usually conducted under laboratory conditions, but the outer environment is significantly different than the laboratory environment, especially due to the severe fluctuations of pH and temperature. These factors can cause significant impact on the adsorption process. Therefore, pilot-scale testing will be crucial for determining the efficiency and stability of MSW biochar and their composites for the remediation of antibiotic residues in aqueous media.

Acknowledgement

Financial support as the grant ASP/01/RE/SCI/2017/83 from the Research Council, University of Sri Jayewardenepura, Sri Lanka, and the analytical support from the Instrument Center, Faculty of Applied Sciences, University of Sri Jayewardenepura, Sri Lanka, are acknowledged.

Appendix A. Supplementary data

Supplementary data to this article can be found online at https://doi.org/10.1016/j.jenvman.2019.02.069.

References

Abdulghani, A.J., Jasim, H.H., Hassan, A.S., 2013. Determination of tetracycline in pharmaceutical preparation by molecular and atomic absorption spectrophotometry and high performance liquid chromatography via complex formation with Au(III) and Hg(II) Ions in solutions. Int. J. Anal. Chem. 2013, 11.

Ahmad, M., Rajapaksha, A.U., Lim, J.E., Zhang, M., Bolan, N., Mohan, D., Vithanage, M., Lee, S.S., Ok, Y.S., 2014. Biochar as a sorbent for contaminant management in soil and water: a review. Chemosphere 99, 19–33.

Anderson, N., Jones, J.G., Page-Dumroese, D., McCollum, D., Baker, S., Loeffler, D., Chung, W., 2013. A comparison of producer gas, biochar, and activated carbon from two distributed scale thermochemical conversion systems used to process forest biomass. Energies 6.

Aristilde, L., Lanson, B., Miéhé-Brendlé, J., Marichal, C., Charlet, L., 2016. Enhanced interlayer trapping of a tetracycline antibiotic within montmorillonite layers in the presence of Ca and Mg. J. Colloid Interface Sci. 464, 153–159.

Chang, P.H., Li, Z., Jean, J.S., Jiang, W.T., Wu, Q., Kuo, C.Y., Kraus, J., 2014. Desorption of tetracycline from montmorillonite by aluminum, calcium, and sodium: an indication of intercalation stability. Int. J. Environ. Sci. Technol. 11, 633–644.

Chang, P.-H., Jiang, W.-T., Li, Z., Kuo, C.-Y., Wu, Q., Jean, J.-S., Lv, G., 2016. Interaction of ciprofloxacin and probe compounds with palygorskite PFl-1. J. Hazard Mater. 303, 55–63.

Chen, F., Yang, X., Mak, H.K.C., Chan, D.W.T., 2010. Photocatalytic oxidation for antimicrobial control in built environment: a brief literature overview. Build. Environ. 45, 1747–1754.

Chen, L., Chen, X.L., Zhou, C.H., Yang, H.M., Ji, S.F., Tong, D.S., Zhong, Z.K., Yu, W.H., Chu, M.Q., 2017. Environmental-friendly montmorillonite-biochar composites: facile production and tunable adsorption-release of ammonium and phosphate. J. Clean. Prod. 156, 648–659.

Chen, T., Luo, L., Deng, S., Shi, G., Zhang, S., Zhang, Y., Deng, O., Wang, L., Zhang, J., Wei, L., 2018. Sorption of tetracycline on H3PO4 modified biochar derived from rice straw and swine manure. Bioresour. Technol. 267, 431–437.

Daghrir, R., Drogui, P., 2013. Tetracycline antibiotics in the environment: a review. Environ. Chem. Lett. 11, 209–227.

Eliopoulos, G.M., Roberts, M.C., 2003. Tetracycline therapy: update. Clin. Infect. Dis. 36, 462–467.

Fosso-Kankeu, E., Waanders, F.B., Steyn, F.W., 2015. The preparation and characterization of clay-biochar composites for the removal of metal pollutants. In: 7th International Conference on Latest Trends in Engineering & Technology, Irene, Pretoria (South Africa).

Halling-Sørensen, B., 2000. Algal toxicity of antibacterial agent used in intensive farming. Chemosphere 40, 731–739.

Han, X., Liang, C.-f., Li, T.-q., Wang, K., Huang, H.-g., Yang, X.-e., 2013. Simultaneous removal of cadmium and sulfamethoxazole from aqueous solution by rice straw biochar. J. Zhejiang Univ. - Sci. B 14, 640–649.

Ho, Y.S., McKay, G., 1998a. Sorption of dye from aqueous solution by peat. Chem. Eng. J. 70, 115–124.

Ho, Y.S., McKay, G., 1998b. A comparison of chemisorption kinetic models applied to pollutant removal on various sorbents. Process Saf. Environ. Protect. 76, 332–340.

Ho, Y.-S., McKay, G., 2002. Application of kinetic models to the sorption of copper(II) on

to peat. Adsorpt. Sci. Technol. 20, 797–815.
Huang, L., Wang, M., Shi, C., Huang, J., Zhang, B., 2014. Adsorption of tetracycline and ciprofloxacin on activated carbon prepared from lignin with H3PO4 activation. Desalination and Water Desalination Water Treat. 52, 2678–2687.
Jang, H.M., Yoo, S., Choi, Y.-K., Park, S., Kan, E., 2018. Adsorption isotherm, kinetic modeling and mechanism of tetracycline on Pinus taeda-derived activated biochar. Bioresour. Technol. 259, 24–31.
Ji, K., Choi, K., Lee, S., Park, S., Khim, J.S., Jo, E.-H., Choi, K., Zhang, X., Giesy, J.P., 2010. Effects of sulfathiazole, oxytetracycline and chlortetracycline on steroidogenesis in the human adrenocarcinoma (H295R) cell line and freshwater fish Oryzias latipes. J. Hazard Mater. 182, 494–502.
Jing, X.-R., Wang, Y.-Y., Liu, W.-J., Wang, Y.-K., Jiang, H., 2014. Enhanced adsorption performance of tetracycline in aqueous solutions by methanol-modified biochar. Chem. Eng. J. 248, 168–174.
Košutić, K., Dolar, D., Ašperger, D., Kunst, B., 2007. Removal of antibiotics from a model wastewater by RO/NF membranes. Separ. Purif. Technol. 53, 244–249.
Koyuncu, I., Arikan, O.A., Wiesner, M.R., Rice, C., 2008. Removal of hormones and antibiotics by nanofiltration membranes. J. Membr. Sci. 309, 94–101.
Krupskaya, V., Zakusin, S., Tyupina, E., Dorzhieva, O., Zhukhlistov, A., Belousov, P., Timofeeva, M., 2017. Experimental study of montmorillonite structure and transformation of its properties under treatment with inorganic acid solutions. Minerals 7, 49.
Lee, H., Lee, E., Lee, C.-H., Lee, K., 2011. Degradation of chlorotetracycline and bacterial disinfection in livestock wastewater by ozone-based advanced oxidation. J. Ind. Eng. Chem. 17, 468–473.
Lehmann, J., Joseph, S., 2009. Biochar for Environmental Management: Science and Technology. Earthscan, UK.
Li, Z., Kolb, V., Jiang, W.-T., Hanlie, H., 2010. FTIR and XRD investigations of tetracycline intercalation in smectites. Clay Clay Miner. 58, 462–474.
Li, Y., Wang, Z., Xie, X., Zhu, J., Li, R., Qin, T., 2017. Removal of norfloxacin from aqueous solution by clay-biochar composite prepared from potato stem and natural attapulgite. Colloid. Surf. Physicochem. Eng. Asp. 514, 126–136.
Liyanage, G., Manage, P., 2017. Risk of prophylactic antibiotics in livestock and poultry farms; a growing problem for human and animal health. Pharm. J. Sri Lanka 7, 13–22.
López-Peñalver, J.J., Sánchez-Polo, M., Gómez-Pacheco, C.V., Rivera-Utrilla, J., 2010. Photodegradation of tetracyclines in aqueous solution by using UV and UV/H2O2 oxidation processes. J. Chem. Technol. Biotechnol. 85, 1325–1333.
Mandal, S., Sarkar, B., Bolan, N., Novak, J., Ok, Y.S., Van Zwieten, L., Singh, B.P., Kirkham, M.B., Choppala, G., Spokas, K., Naidu, R., 2016. Designing advanced biochar products for maximizing greenhouse gas mitigation potential. Crit. Rev. Environ. Sci. Technol 46, 1367–1401.
Parolo, M.E., Savini, M.C., Vallés, J.M., Baschini, M.T., Avena, M.J., 2008. Tetracycline adsorption on montmorillonite: pH and ionic strength effects. Appl. Clay Sci. 40, 179–186.
Peng, B., Chen, L., Que, C., Yang, K., Deng, F., Deng, X., Shi, G., Xu, G., Wu, M., 2016. Adsorption of antibiotics on graphene and biochar in aqueous solutions induced by π-π interactions. In: Scientific Report 31920.
Perelomov, L., Sarkar, B., Rahman, M.M., Goryacheva, A., Naidu, R., 2016. Uptake of lead by Na-exchanged and Al-pillared bentonite in the presence of organic acids with different functional groups. Appl. Clay Sci. 119 (Part 2), 417–423.
Rajapaksha, A.U., Vithanage, M., Jayarathna, L., Kumara, C.K., 2011. Natural red earth as a low cost material for arsenic removal: kinetics and the effect of competing ions. Appl. Geochem. 26, 648–654.
Rajapaksha, A.U., Vithanage, M., Weerasooriya, R., Dissanayake, C.B., 2012. Surface complexation of nickel on iron and aluminum oxides: a comparative study with single and dual site clays. Colloid. Surf. Physicochem. Eng. Asp. 405, 79–87.
Rajapaksha, A.U., Vithanage, M., Ahmad, M., Seo, D.-C., Cho, J.-S., Lee, S.-E., Lee, S.S., Ok, Y.S., 2015. Enhanced sulfamethazine removal by steam-activated invasive plant-derived biochar. J. Hazard Mater. 290, 43–50.
Rivera-Utrilla, J., Gómez-Pacheco, C.V., Sánchez-Polo, M., López-Peñalver, J.J., Ocampo-Pérez, R., 2013. Tetracycline removal from water by adsorption/bioadsorption on activated carbons and sludge-derived adsorbents. J. Environ. Manag. 131, 16–24.
Roberts, J.A., Norris, R., Paterson, D.L., Martin, J.H., 2012. Therapeutic drug monitoring of antimicrobials. Br. J. Clin. Pharmacol. 73, 27–36.
Sarmah, A.K., Meyer, M.T., Boxall, A.B.A., 2006. A global perspective on the use, sales, exposure pathways, occurrence, fate and effects of veterinary antibiotics (VAs) in the environment. Chemosphere 65, 725–759.
Segad, M., Jönsson, B., Akesson, T., Cabane, B., 2010. Ca/Na Montmorillonite: Struct.,Forces Swelling Prop. 26, 5782–5790.
Uddin, F., 2008. Clays, nanoclays, and montmorillonite minerals, Metallurgical and Materials Transactions A 39, 2804–2814.
Vithanage, M., Chandrajith, R., Bandara, A., Weerasooriya, R., 2006. Mechanistic modeling of arsenic retention on natural red earth in simulated environmental systems. J. Colloid Interface Sci. 294, 265–272.
Vithanage, M., Chandrajith, R., Weerasooriya, R., 2007. Role of natural red earth in arsenic removal in drinking water – comparison with synthetic gibbsite and goethite. TTrace Met. Other Contam. Environ 9, 587–601.
Vithanage, M., Rajapaksha, A.U., Tang, X., Thiele-Bruhn, S., Kim, K.H., Lee, S.-E., Ok, Y.S., 2014. Sorption and transport of sulfamethazine in agricultural soils amended with invasive-plant-derived biochar. J. Environ. Manag. 141, 95–103.
Vithanage, M., Mayakaduwa, S.S., Herath, I., Ok, Y.S., Mohan, D., 2016. Kinetics, thermodynamics and mechanistic studies of carbofuran removal using biochars from tea waste and rice husks. Chemosphere 150, 781–789.
Wang, H., Zhou, A., Peng, F., Yu, H., Yang, J., 2007. Mechanism study on adsorption of acidified multiwalled carbon nanotubes to Pb(II). J. Colloid Interface Sci. 316, 277–283.
Yang, G., Wu, L., Xian, Q., Shen, F., Wu, J., Zhang, Y., 2016. Removal of Congo red and methylene blue from aqueous solutions by vermicompost-derived biochars. PLoS One 11, e0154562.
Yao, Y., 2013. In: Sorption of Phosphate and Other Contaminants on Biochar and its Environmental Implications. University of Florida.
Yao, Y., Gao, B., Fang, J., Zhang, M., Chen, H., Zhou, Y., Creamer, A.E., Sun, Y., Yang, L., 2014. Characterization and environmental applications of clay–biochar composites. Chem. Eng. J. 242, 136–143.
Zhou, Y., Liu, X., Xiang, Y., Wang, P., Zhang, J., Zhang, F., Wei, J., Luo, L., Lei, M., Tang, L., 2017. Modification of biochar derived from sawdust and its application in removal of tetracycline and copper from aqueous solution: adsorption mechanism and modelling. Bioresour. Technol. 245, 266–273.
Zhu, R., Chen, Q., Zhou, Q., Xi, Y., Zhu, J., He, H., 2016. Adsorbents based on montmorillonite for contaminant removal from water: a review. Appl. Clay Sci. 123, 239–258.